2840–2855 *Nucleic Acids Research, 2019, Vol. 47, No. 6* *Published online 15 January 2019*
doi: 10.1093/nar/gkz006

RNF20/40-mediated eEF1BδL monoubiquitylation stimulates transcription of heat shock-responsive genes

Suna In[1], Yong-In Kim[2], J. Eugene Lee[2] and Jaehoon Kim[1,*]

[1]Department of Biological Sciences, Korea Advanced Institute of Science and Technology, Daejeon 34141, South Korea and [2]Center for Bioanalysis, Korea Research Institute of Standards and Science, Daejeon 34113, South Korea

Received October 16, 2018; Revised December 27, 2018; Editorial Decision January 02, 2019; Accepted January 03, 2019

ABSTRACT

RNF20/40 E3 ubiquitin ligase-mediated histone H2B monoubiquitylation plays important roles in many cellular processes, including transcriptional regulation. However, the multiple defects observed in RNF20-depleted cells suggest additional ubiquitylation targets of RNF20/40 beyond histone H2B. Here, using biochemically defined assays employing purified factors and cell-based analyses, we demonstrate that RNF20/40, in conjunction with its cognate E2 ubiquitin-conjugating enzyme RAD6, monoubiquitylates lysine 381 of eEF1BδL, a heat shock transcription factor. Notably, monoubiquitylation of eEF1BδL increases eEF1BδL accumulation and potentiates recruitment of p-TEFb to the promoter regions of heat shock-responsive genes, leading to enhanced transcription of these genes. We further demonstrate that cooperative physical interactions among eEF1BδL, RNF20/40, and HSF1 synergistically promote expression of heat shock-responsive genes. In addition to identifying eEF1BδL as a novel ubiquitylation target of RNF20/40 and elucidating its function, we provide a molecular mechanism for the cooperative function of distinct transcription factors in heat shock-responsive gene transcription.

INTRODUCTION

Protein ubiquitylation produced by specific E3 ubiquitin ligases plays diverse roles in many cellular events (1). Whereas polyubiquitylation generally directs proteins for degradation by the proteasome complex (1,2), monoubiquitylation promotes non-proteolytic functions by altering certain features of proteins, including their structure, activity, binding partners and/or subcellular localization (2,3). Previous studies have shown that monoubiquitylation is more prevalent than polyubiquitylation in cells (4) and that monoubiquitylation occurs in a reversible manner (5,6), suggesting pivotal regulatory functions of protein monoubiquitylation in cellular processes.

Human RNF20/40 (also called the BRE1 complex), first identified as an E3 ubiquitin ligase for histone H2B (7,8), utilizes RAD6 as a cognate E2 ubiquitin-conjugating enzyme (8). Depletion of RNF20 has been shown to cause various cellular defects in genomic stability, tumor suppression and inflammation, among other effects (9–11). However, it is uncertain whether all these misregulations are caused by defects in H2B ubiquitylation. In support of this, a yeast strain lacking Bre1 (yeast homolog of RNF20 and RNF40) exhibits more severe hypersensitivity to DNA damage than the htb-K123R strain, expressing histone H2B containing an arginine substitution at the site monoubiquitylated by Bre1 (lysine 123) (12), suggesting additional Bre1 target protein(s). Moreover, genome-wide transcriptome analyses have shown that RNF20 knockdown selectively regulates distinct subsets of genes (9), raising the possibility that RNF20/40 regulates transcription through complex mechanisms that are not solely dependent on H2B ubiquitylation.

In this context, several studies have reported non-histone proteins that are polyubiquitylated (13–15) or monoubiquitylated (16) by RNF20/40. However, these cell-based studies do not completely exclude the possibility that RNF20 depletion indirectly affects target protein ubiquitylation by virtue of the presence of various unknown cellular components, emphasizing the necessity of biochemical analyses using defined factors to directly demonstrate RNF20/40-mediated target protein ubiquitylation and function. In addition, given that RNF20/40 ubiquitylates the 'nucleosomal' component histone H2B, it is plausible that RNF20/40 targets additional chromatin-proximal proteins, such as transcription factors. However, no previously studies have identified such proteins.

Here, using biochemically defined systems and cell-based analyses, we demonstrate that RNF20/40 monoubiquitylates eEF1BδL, a heat shock-responsive transcription factor (17). We also provide mechanistic insight into the role of monoubiquitylated eEF1BδL in stimulating heat

*To whom correspondence should be addressed. Tel: +82 42 350 2632; Fax: +82 42 350 2610; Email: kimjaehoon@kaist.edu

shock-responsive gene expression, showing that this process involves cooperative interactions among eEF1BδL, RNF20/40 and HSF1, and recruitment of the transcription elongation factor p-TEFb to the promoter regions of target genes. In addition to elucidating a detailed molecular mechanism of eEF1BδL function in response to thermal stress, our study reveals a non-proteolytic function of RNF20/40-mediated protein monoubiquitylation.

MATERIALS AND METHODS

Plasmids, baculoviruses, recombinant proteins and purifications

Plasmids containing full-length human eEF1BδL, eEF1Bδ1 and HSF1 cDNA, and the pHSE-luc plasmid were obtained from Dr. Masayuki Matsushita at University of the Ryukyus. Expression and purification of N-terminal GST- and His-tagged recombinant proteins in *Escherichia coli* were as described (18). For untagged RAD6A preparation, RAD6A protein with N-terminal His- and MBP (maltose binding protein)-tags followed by TEV cleavage site was expressed in *E. coli* and purified on Ni-NTA agarose (Qiagen). Resulting His-MBP-TEV-RAD6A protein was reacted with purified His-tagged TEV protease and then reaction mixture was incubated with Ni-NTA agarose. Unbound fraction was concentrated to enrich untagged RAD6A. For baculovirus-mediated recombinant protein expression, cDNAs were subcloned into pFASTBAC1 (Gibco-Invitrogen) with or without an epitope tag and baculoviruses were generated according to the manufacturer's instruction**.** FLAG-tagged proteins/complexes were expressed in Sf9 cells and purified on M2 agarose (Sigma-Aldrich) as described (18).

Cell culture and transfection

293T cells were maintained in Dulbecco's modified Eagle's medium (Corning) supplemented with 10% (v/v) fetal bovine serum (FBS) (Atlas), 100 U/ml penicillin (Gibco) and 100 μg/ml streptomycin (Gibco) at 37°C in a 5% CO_2 humidified incubator. For transient transfections, cells were transfected with plasmids by using iN-fect transfection reagent (iNtRON Biotechnology) according to the manufacturer's instruction. For RNA interference, cells were transfected with siRNA oligonucleotides by using DharmaFECT 1 transfection reagent (Dharmacon) according to the manufacturer's protocol. Oligonucleotide sequences for siRNA are summarized in Supplementary Table S1. Sf9 cells were cultured in Grace's insect medium (Gibco) supplemented with 10% (v/v) FBS, 1% (v/v) Pluronic F-68 (Sigma-Aldrich) and 10 μg/ml gentamicin (Gibco) in normal atmospheric conditions.

Immunoprecipitation of RNF20- and RNF40-interacting proteins and liquid chromatography-mass spectrometry

293T cells and its derived cell line that carries chromosomal FLAG-RNF20 and HA-RNF40 genes were lysed in lysis buffer (50 mM HEPES [pH 7.5], 300 mM NaCl, 70 mM KOAc, 5 mM $Mg(OAc)_2$, 0.2% *n*-dodecyl-β-D-maltoside and protease inhibitor cocktail (Roche)) at 4°C for 30 min. Cell lysates were centrifuged at 16,000 × g for 20 min. The supernatant was incubated with M2 agarose or anti-HA agarose (Sigma-Aldrich) beads at 4°C for 2 h. The beads were washed five times with lysis buffer and then twice with mass spectrometry (MS) buffer (100 mM Tris−Cl [pH 8.5]). The bound proteins were eluted from the beads by incubation in 10 M urea at room temperature (RT) for 15 min and then the eluted samples were diluted to 8 M urea by adding the MS buffer. For reduction of proteins, Tris(2-carboxyethyl)-phosphine was added at final 3 mM and incubated at RT for 20 min. To alkylate the cysteine residues, 2-chloro-acetamide was added at final 20 mM and incubated at RT for 15 min. Proteins were digested by Lys-C-endoprotease (Wako) at 37°C for 4 h. Sample solutions were adjusted to 2 M urea and 1 mM $CaCl_2$ before being further digested by trypsin (Promega) at 37°C for 14 h. Reactions were stopped by adding formic acid at final 1% concentration. The digested peptides were desalted on reverse-phased C18 STAGE-Tips (19). The resulting elutes were dried in a vacuum concentrator and resuspended in 0.1% formic acid. All liquid chromatography-mass spectrometry analyses were performed with an EASY-nLC™ 1000 coupled to the Q-Exactive™ Orbitrap mass spectrometer (Thermo Scientific) equipped with a custom electrospray ionization source. Digested peptides were separated on a 150-mm reversed phase analytical column (75-μm internal diameter) packed with C18 AQ resin (3 μm, 10 nm) (Bonna-Agela Technologies). This separation took 130 min with a gradient of 2–95% acetonitrile at a flow rate 350 nl/min. The mass spectrometer was automatically switched between full-scan MS and tandem MS acquisition in data-dependent mode. Full-scan survey mass spectra were collected with an Orbitrap (300–1,800 m/z) utilizing an automated gain control target of 3 million ions with a resolution of 70,000. Tandem mass spectra were acquired using an automated gain control target of a half-million ions with a resolution of 17,500. Top 12 most intense ions were isolated for fragmentation by higher-energy collisional dissociation. Screening for precursor ion charged states was conducted and all single- and unassigned-charged states were rejected.

Mass spectrometry data analysis

MS peaks were generated from MS raw files using MaxQuant (version 1.6.1.0). The Andromeda peptide search engine in MaxQuant was used to match the MS peaks against a concatenated Uniprot human database (2018.4.28. version) and a decoy database with modified reversing of protein sequences as described previously (20). The search parameters were trypsin digestion, fixed carboxyamidomethyl modifications of cysteine, maximum of two missed cleavages, variable oxidation of methionine, variable acetylation of protein N-termini and variable carbamylation of peptide N-termini. Mass tolerance was 4.5 ppm and 20 ppm for precursor and fragment ions, respectively. Protein inference and quantitation were performed using MaxQuant with a 1% false discovery rate threshold for both peptides and proteins. Abundances of the identi-

fied proteins were inferred from the iBAQ (intensity based absolute quantification) values (21).

In vitro protein interaction assays

For GST-pull down assays, 2 μg of GST-tagged proteins immobilized on glutathione-Sepharose 4B beads (GE Healthcare) were incubated with 200 ng of purified proteins in binding buffer (20 mM Tris−Cl [pH 7.9], 150 mM KCl, 0.2 mM EDTA, 20% glycerol, 0.05% NP-40 and 0.2 mg/ml BSA) at 4°C for 3 h. For FLAG-pull down assays, 1 μg of FLAG-tagged proteins immobilized on M2 agarose were incubated with 200 ng of purified proteins in binding buffer (20 mM Tris−Cl [pH 7.9], 150 mM KCl, 0.2 mM EDTA, 20% glycerol, 0.05% NP-40 and 0.5 mg/ml BSA) at 4°C for 3 h. For His-pull down assays, 2 μg of His-tagged proteins immobilized on Ni-NTA agarose were incubated with 200 ng of purified proteins in binding buffer (20 mM Tris−Cl [pH 7.9], 150 mM KCl, 0.2 mM EDTA, 20% glycerol, 0.05% NP-40 and 0.2 mg/ml BSA) at 4°C for 3 h. Beads were extensively washed with the binding buffer used for each assay (without BSA) and bound proteins were scored by immunoblotting.

In vitro ubiquitylation assays

Reactions containing 100 ng E1, 2.8 μg His-pK-HA-ubiquitin (pK indicates a protein kinase recognition site), 480 ng eEF1BδL and combination of E2 and E3 proteins (200 ng RAD6A, 600 ng RNF20/40 or 660ng RNF20/40−RAD6A complex) in 25 μl reaction buffer (50 mM Tris−Cl [pH 7.9], 5 mM $MgCl_2$, 2 mM NaF, 0.4 mM DTT and 4 mM ATP) were incubated at 37°C for 1 h, resolved by SDS-PAGE and subjected to immunoblot analysis.

Heat shock treatments

For assays involving heat shock treatment, cells were incubated at 42°C for 1 h or 90 min and allowed to recover at 37°C for varying times depending on assays. Recovery time that shows most significant effect in each assay was empirically determined. Specific heat shock treatment conditions for each assay are described below.

Co-immunoprecipitation assays

For co-immunoprecipitation of endogenous proteins, cells were lysed in lysis buffer (20 mM Tris−Cl [pH 7.9], 150 mM KCl, 0.2 mM EDTA, 20% glycerol, 0.1% NP-40 and 1 mM PMSF) and cell extracts were incubated with the antibody at 4°C for overnight. After addition of Protein A/G PLUS-Agarose (Santa Cruz Biotechnology), reactions were further incubated at 4°C for 3 h. For co-immunoprecipitation with FLAG-tagged proteins, 293T cells were transfected with combinations of expression plasmids. After 2 days, cells were lysed in lysis buffer and cell extracts were incubated with M2 agarose at 4°C for 2 h. Beads were extensively washed with the lysis buffer and bound proteins were monitored by immunoblotting. For assays involving heat shock treatment, cells were incubated at 42°C for 90 min, allowed to recover at 37°C for 19 h, and then were subjected to co-immunoprecipitation.

In vivo ubiquitylation assays

Approximately 5×10^5 293T cells were transfected with combinations of 1 μg FLAG-eEF1BδL, 500 ng HA-ubiquitin, 500 ng RNF20 and 500 ng RNF40 expression plasmids as indicated and grown for 2 days. For detection of ubiquitylated proteins by anti-FLAG antibody, cells were lysed in lysis buffer (20 mM Tris−Cl [pH 7.9], 300 mM KCl, 0.2 mM EDTA, 20% glycerol, 0.1% NP-40 and 1 mM PMSF). For detection of ubiquitylated proteins by anti-HA antibody, cells were lysed in lysis buffer (20 mM Tris−Cl [pH 7.9], 1 M KCl, 0.2 mM EDTA, 20% glycerol, 1% NP-40 and 1 mM PMSF). FLAG-tagged and HA-tagged proteins were captured by incubation of cell extracts with M2 agarose and anti-HA agarose (Pierce), respectively, at 4°C for 2 h. Beads were washed with lysis buffer used for each assay and bound proteins were scored by immunoblotting. For the assays involving heat shock treatment, cells were incubated at 42°C for 1 h, allowed to recover at 37°C for 3 h, and then were subjected to ubiquitylation analysis.

Luciferase assays

About 10^5 293T cells were transfected with 25 ng luciferase reporter plasmid and combinations of 50 ng eEF1BδL, 25 ng RNF20 and 25 ng RNF40 expression plasmids as indicated. After 2 days, cells were harvested and analyzed for luciferase activity using luciferase assay kit (Biotium).

Quantitative RT-PCR analyses

Total RNA was extracted using an RNA-spin total RNA extraction kit (iNtRON Biotechnology), and contaminating genomic DNA was removed by treatment with DNase I (NEB). cDNA was synthesized by reverse transcription using a PrimeScript RT Master Mix (Takara), and RT-qPCR was performed using TOPreal qPCR PreMIX (Enzynomics). Primers for qPCR reactions are summarized in Supplementary Table S2. The data analysis was performed by calculating ΔCq normalized to β-actin expression by the Bio-Rad CFX Manager 3.1 based on the MIQE guidelines (22). The MIQE checklist is provided in Supplementary Table S4. For assays involving heat shock treatment, cells were incubated at 42°C for 1 h, allowed to recover at 37°C for 3 h, and then were subjected to RT-qPCR analysis. For assays involving both siRNA and heat shock treatments, cells were incubated at 42°C for 1 h, allowed to recover at 37°C for 18 h, and then were subjected to RT-qPCR analysis.

Chromatin immunoprecipitation assays

ChIP analyses were performed according to the manufacturer's instruction (Millipore). Briefly, cells were treated with 1% formaldehyde at 37°C for 10 min for crosslinking. Cell lysates prepared by sonication in lysis buffer were subjected to immunoprecipitation with antibodies at 4°C

for overnight. After addition of Protein A agarose and further incubation at 4°C for 4 h, beads were extensively washed with wash buffers. Immunoprecipitated complexes were eluted with elution buffer, the protein-DNA complexes were reversed by incubation at 65°C for overnight. DNA was purified by phenol/chloroform extraction and enrichment of DNA was measured by qPCR analysis. Primers for qPCR reactions are summarized in Supplementary Table S3. Percentage input was calculated by equation of $2^{(Cq(Input)-Cq(IP))} \times 100$. Cq is the quantification cycle as calculated by the Bio-Rad CFX Manager 3.1 based on the MIQE guidelines (22). The MIQE checklist is provided in Supplementary Table S5. For assays involving heat shock treatment, cells were incubated at 42°C for 1 h and then were subjected to ChIP analyses without recovery at 37°C to monitor rapid recruitment of proteins to the promoter regions of the genes upon heat shock.

Antibodies

Polyclonal anti-RNF20 (23) and anti-RNF40 (8) antibodies were described. The following antibodies were obtained commercially: anti-FLAG (Sigma-Aldrich); anti-GST, anti-β-actin and anti-HA for immunoblot analysis (Santa Cruz Biotechnology); anti-RNF20, anti-H2B and anti-HA for ChIP assay (Abcam); anti-CDK9 and anti-UbH2BK120 (Cell Signaling Technology); anti-eEF1BδL (Proteintech Group); anti-HSF1 (Enzo Life Sciences); anti-Ubiquitin (Dako).

RESULTS

RNF20/40 directly interacts with eEF1BδL

In protein ubiquitylation systems, an E3 ubiquitin ligase recognizes and directly interacts with its target protein (1). To screen for novel ubiquitylation target protein(s) of the RNF20/40 E3 ubiquitin ligase, we performed FLAG and HA pull-downs independently using cell extracts derived from a 293T cell line expressing FLAG-RNF20 and HA-RNF40 from chromosome-integrated genes (Supplementary Figure S1A) and identified interacting proteins by mass spectrometric analysis (Supplementary Table S6). Among proteins topping the interactome list in FLAG-RNF20 and HA-RNF40 immunoprecipitates were RNF40 and RNF20 (7,8), respectively. In addition, these analyses identified RAD6A, a cognate E2 ubiquitin-conjugating enzyme of RNF20/40 (8), and WAC, a regulator of transcription-coupled histone H2B ubiquitylation (24),—both of which are known to interact with RNF20/40 (Supplementary Figure S1B).

In addition to identifying these proteins, which validated our screening approach, our mass spectrometric analysis also identified eEF1Bδ as a potential candidate interacting protein of RNF20/40. In humans, eEF1Bδ is present in two isoforms, eEF1Bδ1 and eEF1BδL, that are products of alternatively spliced transcripts of the *EEF1D* gene (25) (Figure 1A, Supplementary Figure S1B). Cytoplasmic eEF1Bδ1 represents one of the four subunits that constitute the eEF1B translation-elongation complex (25,26). Inclusion of an additional exon in eEF1Bδ1 mRNA results in the longer isoform, eEF1BδL, which contains a nuclear localization sequence (NLS) in its N-terminal region (Figure 1A), suggesting a nuclear function rather than a role in the cytoplasmic translation process (25). In support of this, it has been reported that eEF1BδL, but not eEF1Bδ1, functions as a heat shock-responsive transcription factor (17). Accordingly, we postulated that RNF20/40 might regulate the function of eEF1BδL in heat shock-responsive gene expression.

To determine whether eEF1BδL directly interacts with RNF20/40, we performed GST pull-down assays using purified FLAG-eEF1BδL and GST-RNF20/FLAG-RNF40 proteins (Supplementary Figure S1C). These assays revealed that eEF1BδL directly interacted with RNF20/40 *in vitro* (Figure 1B). To determine the regions of eEF1BδL responsible for the interaction with RNF20/40, we purified GST-tagged eEF1BδL fragments (Figure 1C, Supplementary Figure S1D) and tested their interaction with purified FLAG-RNF20/RNF40 protein (Supplementary Figure S1C). This analysis demonstrated selective binding of RNF20/40 to two N-terminal fragments encompassing amino acid residues 1–367 of eEF1BδL (Figure 1D).

In a test of intracellular interactions, we found that an anti-eEF1BδL antibody co-immunoprecipitated endogenous RNF20 (Figure 1E, left). In a reciprocal approach, an anti-RNF20 antibody was shown to selectively enrich endogenous eEF1BδL, but importantly, not eEF1Bδ1 (Figure 1E, right). (Note that the anti-eEF1BδL antibody recognizes both eEF1BδL and eEF1Bδ1 because it was developed against amino acid residues 347–647 of eEF1BδL.) Co-immunoprecipitation with an anti-eEF1BδL antibody after heat shock treatment resulted in slightly enhanced level of RNF20 immunoprecipitation relative to input (Supplementary Figure S1E), suggesting that heat shock might potentiate eEF1BδL-RNF20/40 interaction. In a further confirmation using ectopically expressed FLAG-RNF20, RNF40 and HA-eEF1BδL fragments, RNF20/40 showed a selective interaction with the N-terminus of eEF1BδL (Figure 1F, Supplementary Figure S1F). Collectively, these results indicate that RNF20/40 directly interacts with the N-terminal region of eEF1BδL. Based on the nuclear localization and functions of RNF20/40 (23), these observations raise the possibility that RNF20/40 regulates the function of eEF1BδL in the nucleus.

RNF20/40 and RAD6 mediate monoubiquitylation of eEF1BδL at lysine 381

Given the demonstration of a direct RNF20/40-eEF1BδL interaction and the known E3 ubiquitin ligase activity of RNF20/40, we investigated the possibility that eEF1BδL can be ubiquitylated by RNF20/40. To test this, we employed an *in vitro* ubiquitylation assay using purified factors, a previously established approach for studying nucleosomal histone H2B ubiquitylation (8,18). In this assay, purified human E1, RAD6A, RNF20/40 and eEF1BδL (Supplementary Figure S2A) served as E1 ubiquitin-activating enzyme, E2 ubiquitin-conjugating enzyme, E3 ubiquitin ligase and ubiquitylation substrate, respectively, and ubiquitylation of eEF1BδL was monitored by immunoblotting with anti-eEF1BδL and anti-Ubiquitin antibodies. Complete re-

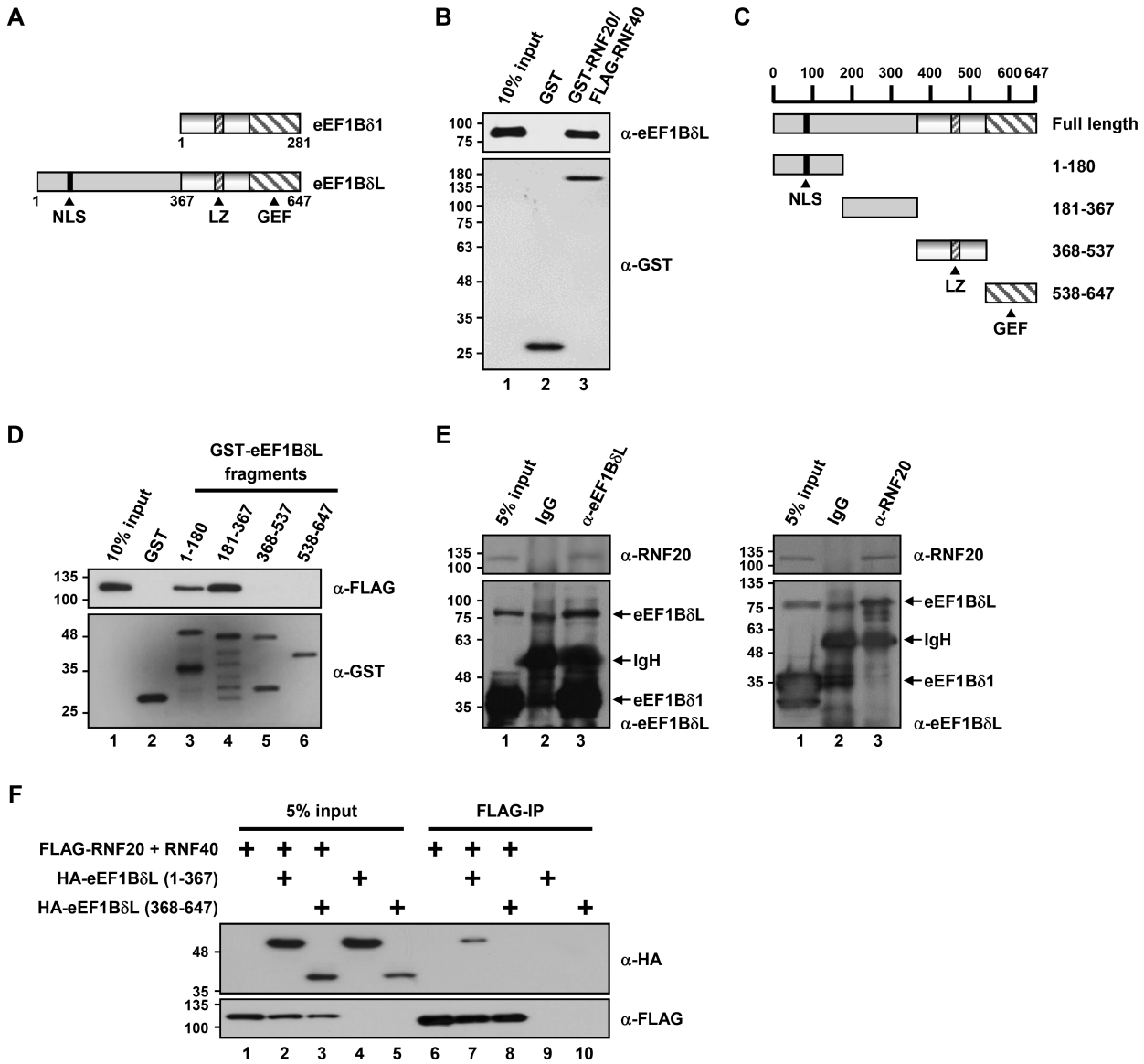

Figure 1. RNF20/40 directly interacts with eEF1BδL. (**A**) A schematic diagram of human eEF1Bδ1 and eEF1BδL with predicted NLS (nuclear localization sequence), LZ (leucine zipper) and GEF (guanine nucleotide exchange factor) domains. (**B**) Direct binding of eEF1BδL to RNF20/40. GST pull-down assays employed purified GST-RNF20/FLAG-RNF40 and FLAG-eEF1BδL (Supplementary Figure S1C). The bound proteins were scored by immunoblotting with the indicated antibodies. (**C**) A schematic diagram of eEF1BδL-derived fragments with predicted domains. Note that because of the absence of any identified motif, the fragment encoding eEF1BδL residues 181–367 is depicted as blank box. (**D**) Direct binding of RNF20/40 to the N-terminal region of eEF1BδL. Purified FLAG-RNF20/RNF40 (Supplementary Figure S1C) was tested for binding to GST-eEF1BδL fragments (Supplementary Figure S1D). (**E**) Intracellular interaction between RNF20 and eEF1BδL. Cell extracts derived from 293T cells were immunoprecipitated with anti-eEF1BδL (left) and anti-RNF20 (right) antibodies, and the bound proteins were monitored by immunoblotting with the indicated antibodies. (**F**) Intracellular interaction of RNF20 with the N-terminal region of eEF1BδL. 293T cells were co-transfected with plasmids expressing FLAG-RNF20, RNF40 and HA-eEF1BδL fragments as indicated. Cell extracts were immunoprecipitated with M2 agarose (FLAG-IP), and the bound proteins were visualized by immunoblotting with the indicated antibodies.

actions containing E1, RAD6A, RNF20/40, ubiquitin and eEF1BδL generated ubiquitylated eEF1BδL (Figure 2A, lanes 2 and 8), whereas reactions lacking E1, RAD6A, ubiquitin, or eEF1BδL did not (Figure 2A, lanes 3, 4, 6 and 7). Notably, we found that eEF1BδL ubiquitylation was still observed in a reaction lacking RNF20/40 (Figure 2A, lane 5). This E3-independent ubiquitylation of eEF1BδL might reflect nonspecific ubiquitin-conjugating activity of RAD6, which manifests in a purified system, as previously shown for RAD6-mediated ubiquitylation of histones *in vitro* in the absence of RNF20/40 (8,27,28). In a related observation, it has been reported that formation of a complex of RAD6 with RAD18 inhibits the ubiquitin chain formation activity of RAD6 and directs RAD6 toward the specific monoubiquitylation site of PCNA (proliferating cell nuclear antigen) (29). In light of these observations, we sought to clarify the requirement of RNF20/40 for eEF1BδL ubiquitylation by recon-

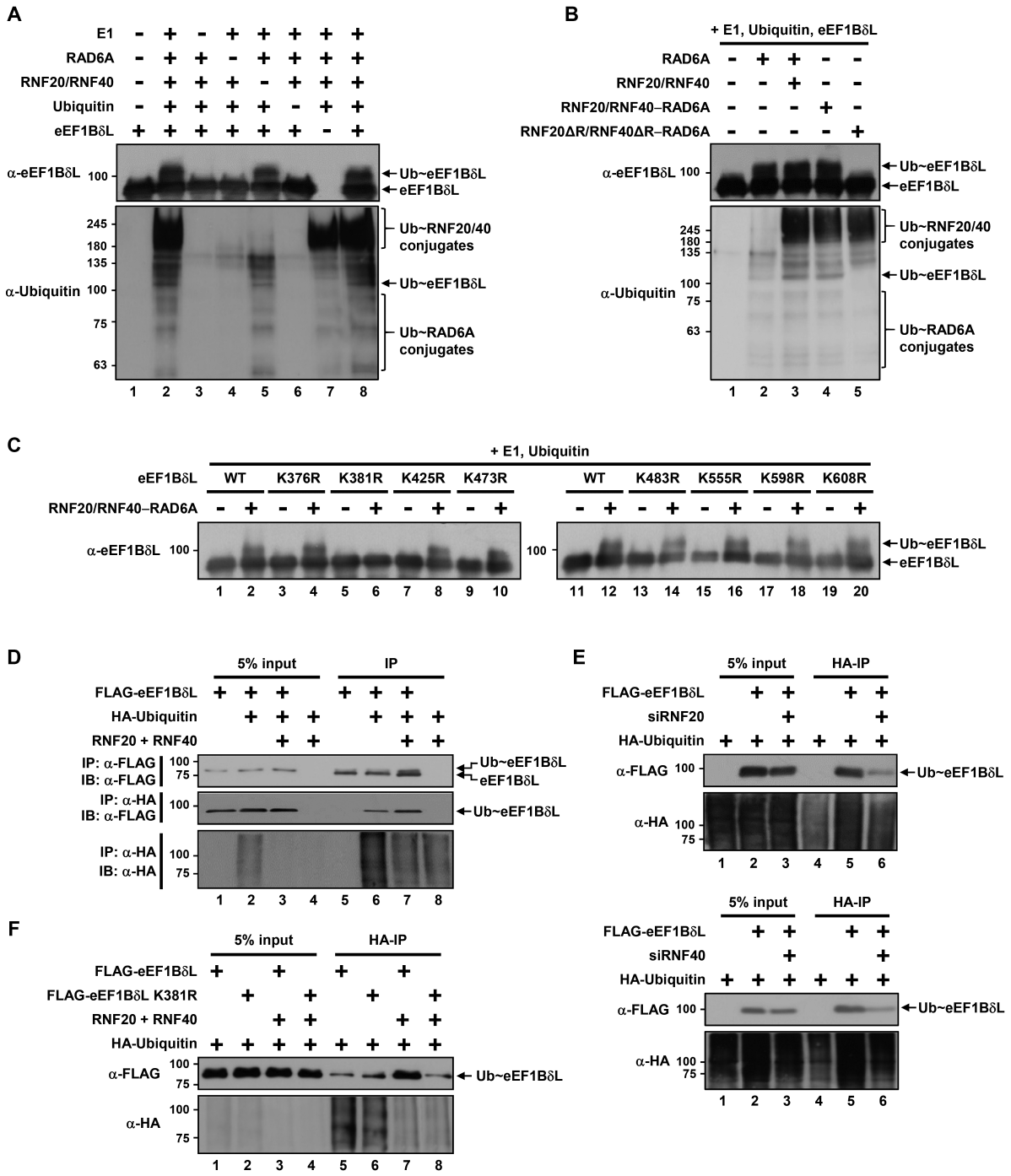

Figure 2. RNF20/40 and RAD6 mediate monoubiquitylation of eEF1BδL at lysine 381. (**A**) Collective requirement of factors for eEF1BδL ubiquitylation. The *in vitro* ubiquitylation reactions containing the indicated combinations of purified human FLAG-E1, untagged RAD6A, FLAG-RNF20/RNF40, His-pK-HA-Ubiquitin (pK indicates a protein kinase recognition site) and FLAG-eEF1BδL (Supplementary Figure S2A) were subjected to immunoblot analyses with anti-eEF1BδL and anti-Ubiquitin antibodies. Monoubiquitylated eEF1BδL (Ub~eEF1BδL), polyubiquitylated RAD6A (Ub~RAD6A conjugates) and polyubiquitylated RNF20/40 (Ub~RNF20/40 conjugates) are indicated. (**B**) Requirement of RNF20/40 for eEF1BδL monoubiquitylation. Purified RAD6A, FLAG-RNF20/RNF40, FLAG-RNF20/RNF40–RAD6A and FLAG-RNF20ΔR/RNF40ΔR–RAD6A were added, as indicated, to *in vitro* eEF1BδL ubiquitylation assays. (**C**) RNF20/40- and RAD6A-mediated monoubiquitylation at lysine 381 of eEF1BδL *in vitro*. Purified wild-type and mutant eEF1BδL proteins (Supplementary Figure S2H) were tested in an *in vitro* ubiquitylation assay employing FLAG-RNF20/RNF40–RAD6A. (**D** and **F**) RNF20/40-mediated eEF1BδL monoubiquitylation at lysine 381 in cells. 293T cells were co-transfected with FLAG-eEF1BδL (D), either wild-type or K381R FLAG-eEF1BδL (F) and RNF20, RNF40, HA-ubiquitin expression plasmids as indicated. Cell extracts were immunoprecipitated with M2 agarose or anti-HA agarose (HA-IP) as indicated and subjected to immunoblot analyses with the indicated antibodies. IP, immunoprecipitation; IB, immunoblot. (**E**) Requirements of endogenous RNF20 and RNF40 for eEF1BδL monoubiquitylation in cells. 293T cells treated with RNF20- (siRNF20, top) or RNF40-targeted (siRNF40, bottom) siRNAs were co-transfected with FLAG-eEF1BδL and HA-ubiquitin expression plasmids as indicated. Cell extracts were immunoprecipitated with anti-HA agarose and eEF1BδL ubiquitylation levels were scored by immunoblotting with anti-FLAG antibody.

stituting RNF20/40−RAD6A complexes in Sf9 insect cells using baculovirus-mediated expression of FLAG-RNF20, RNF40 and RAD6A (Supplementary Figure S2B). We found that RAD6A complexed with RNF20ΔR/40ΔR, a RING finger domain-deletion mutant, showed no ubiquitylation activity toward eEF1BδL (Figure 2B, lane 5) or nucleosomal histone H2B (Supplementary Figure S2C), indicating that the nonspecific ubiquitin-conjugating activity of RAD6 is suppressed by complex formation with RNF20/40 and that RING finger domains within RNF20/40 are required for ubiquitylation of eEF1BδL. In contrast, RAD6A complexed with RNF20/40 exerted significant ubiquitylation activity toward eEF1BδL (Figure 2B, lane 4), producing a level of ubiquitylated eEF1BδL comparable to that produced by separate addition of RNF20/40 and RAD6A (Figure 2B, lane 3). In a test for contribution of individual RING finger domains for E3 ubiquitin ligase activity, both purified RNF20ΔR/40−RAD6A and RNF20/40ΔR−RAD6A complexes (Supplementary Figure S2D) generated reduced levels of eEF1BδL (Supplementary Figure S2E) and nucleosomal histone H2B (Supplementary Figure S2F) ubiquitylation compared to RNF20/40−RAD6A complex, indicating redundant but essential functions of two RING finger domains for full E3 ubiquitin ligase activity of RNF20/40. Taken together, these analyses unequivocally identify the factors that are necessary and sufficient for eEF1BδL ubiquitylation *in vitro*. Importantly, we further observed a slower-migrating species in all immunoblot analyses that appeared as a single band, suggesting that RNF20/40 and RAD6A mediate monoubiquitylation of eEF1BδL at a single site.

Several proteome-wide mass spectrometric studies have reported that eEF1BδL is ubiquitylated *in vivo* and also identified several potential ubiquitylation sites, mostly within the C-terminal half of eEF1BδL (6,30,31) (Supplementary Figure S2G). To identify the specific site on eEF1BδL that is ubiquitylated by RNF20/40 and RAD6, we purified eEF1BδL mutant proteins in which each individual lysine residue proposed to be ubiquitylated in cells (6,30,31) was replaced with arginine (Supplementary Figure S2H), and used them in *in vitro* ubiquitylation assays with RNF20/40−RAD6A complex (Figure 2C). These assays showed that monoubiquitylation of eEF1BδL disappeared only in the reaction containing the K381R mutant (Figure 2C, lane 6), indicating that RNF20/40 directs RAD6A-mediated ubiquitylation specifically at lysine 381 of eEF1BδL.

To test whether eEF1BδL is ubiquitylated by RNF20/40 in cells, we co-transfected 293T cells with FLAG-eEF1BδL, HA-ubiquitin, RNF20 and RNF40 expression plasmids. Cell lysates were immunoprecipitated with M2 agarose, and ubiquitylation of eEF1BδL was monitored by immunoblotting with an anti-FLAG antibody. eEF1BδL was modified with ubiquitin, as evidenced by the detection of a slowly migrated band, presumably ubiquitylated eEF1BδL (Figure 2D, top, lane 6), whose level was increased by overexpression of RNF20/40 (Figure 2D, top, lane 7 versus lane 6). To confirm that the slow-migrating band was indeed ubiquitylated eEF1BδL, we immunoprecipitated cell lysates with an anti-HA antibody under high-stringency conditions to enrich ubiquitylated proteins, and monitored ubiquitylation of eEF1BδL by immunoblotting using an anti-FLAG antibody. This approach confirmed ubiquitylation of eEF1BδL in cells (Figure 2D, middle, lane 6), and showed that it was increased by RNF20/40 (Figure 2D, middle, lane 7 versus lane 6).

To determine whether endogenous RNF20 and RNF40 are essential for eEF1BδL ubiquitylation, we performed RNA interference experiments in 293T cells. We found that transfection of a small interfering RNA (siRNA) targeting RNF20 or RNF40 resulted in efficient and concomitant decrease in intracellular RNF20 and RNF40 protein levels (Supplementary Figure S2I), highlighting the importance of complex formation of RNF20 and RNF40 for their stabilization in cells, and significantly reduced eEF1BδL ubiquitylation (Figure 2E, lane 6 versus lane 5, Supplementary Figure S2J). Next, we tested the site specificity of RNF20/40-mediated eEF1BδL ubiquitylation in cells. We found that no RNF20/40-dependent increase in eEF1BδL ubiquitylation was observed using the eEF1BδL K381R mutant (Figure 2F, top, lane 8 versus lane 7, Supplementary Figure S2K), which retains the ability to interact with RNF20/40 (Supplementary Figure S2L), confirming that RNF20/40 promotes ubiquitylation of eEF1BδL at lysine 381 in cells. Although we did note persistent ubiquitylation of the eEF1BδL K381R mutant (Figure 2F, top, lanes 6 and 8), this might reflect the presence of additional E3 ubiquitin ligases that target residues other than K381, as suggested by previous proteome-wide analyses (6,30,31). Collectively, our analyses clearly demonstrate that RNF20/40, in conjunction with RAD6, monoubiquitylates lysine 381 of eEF1BδL *in vitro* and in cells.

RNF20/40 enhances eEF1BδL-dependent expression of heat shock-responsive genes

Given that eEF1BδL functions as a heat shock-responsive transcription factor (17) and that the transactivation activity of some transcription factors is regulated by monoubiquitylation (2,3,32), we tested whether expression of heat shock-responsive genes was affected by RNF20/40-dependent eEF1BδL monoubiquitylation. To this end, 293T cells were co-transfected with a luciferase reporter containing multiple copies of the heat shock element (HSE) consensus sequence (17) in combination with RNF20 and RNF40, and eEF1Bδ1, eEF1BδL or eEF1BδL K381R expression plasmids. Consistent with a previous report (17), eEF1BδL increased luciferase activity (Figure 3A, lane 2), whereas eEF1Bδ1 did not (Figure 3A, lane 3). Importantly, RNF20/40 significantly enhanced eEF1BδL-dependent transcription (Figure 3A, lane 6 versus lane 2) in an RING finger domain-dependent manner (Figure 3A, lane 10 versus lane 6) and this effect was markedly diminished in an assay containing the eEF1BδL K381R mutant (Figure 3A, lane 8 versus lane 6).

To investigate whether RNF20/40 affects transcription of endogenous heat shock-responsive genes, we co-transfected 293T cells with eEF1BδL, RNF20 and RN40 expression plasmids, and measured transcripts of several HSE-containing genes that were previously shown to respond to heat shock (*HSPA6*, *DNAJB1* and *CRYAB*) (33–35) by quantitative reverse transcription-polymerase

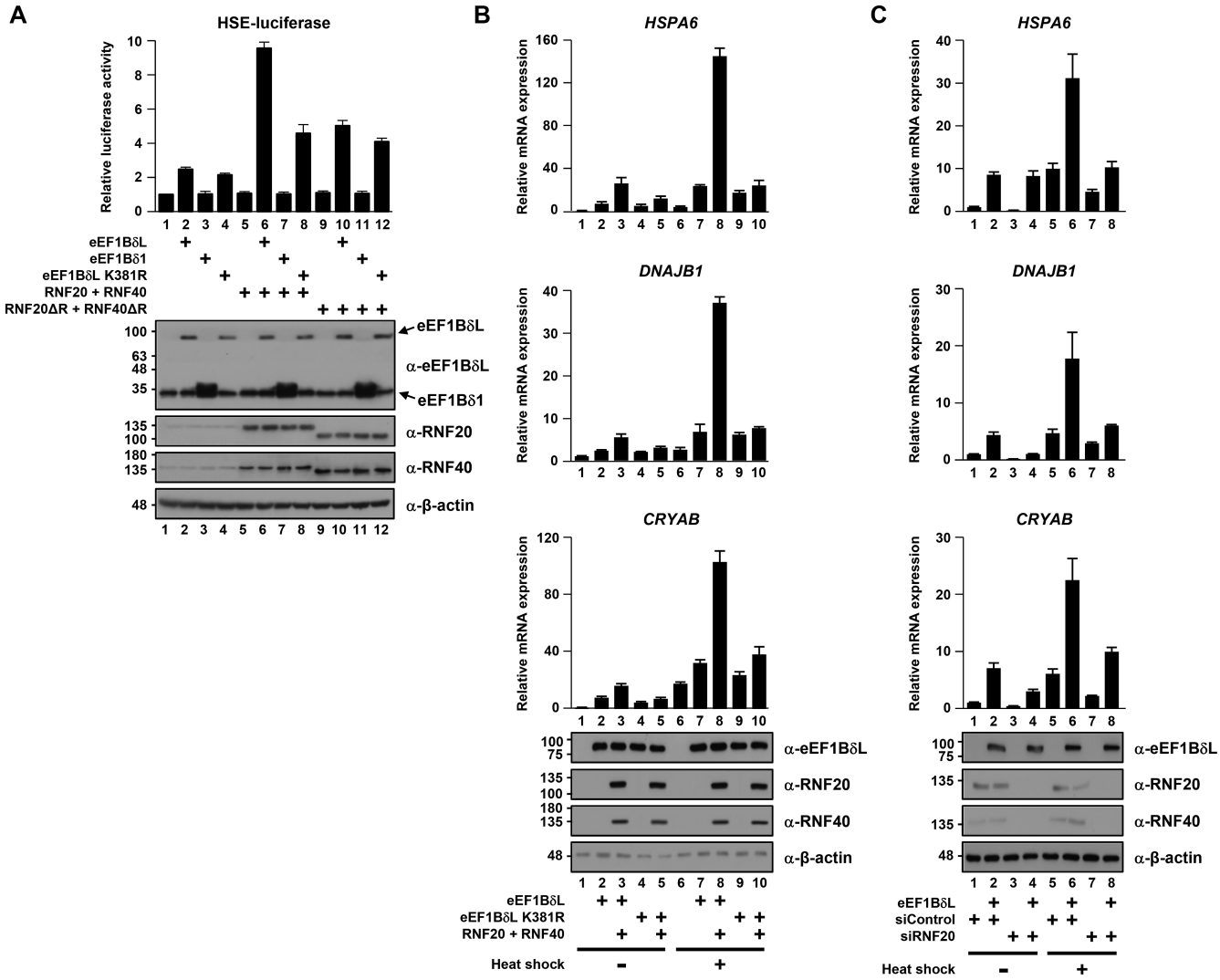

Figure 3. RNF20/40 enhances eEF1BδL-dependent expression of heat shock-responsive genes. (**A**) 293T cells were co-transfected with a luciferase reporter containing the HSE (heat shock element) consensus sequences and eEF1BδL and RNF20/40 expression plasmids as indicated. Cell extracts were subjected to luciferase analyses. (**B** and **C**) 293T cells were co-transfected with indicated protein expression plasmids (B). 293T cells treated with either control (siControl) or RNF20-targeted siRNAs were transfected with eEF1BδL expression plasmid as indicated (C). After heat shock treatment where indicated, mRNA levels of the *HSPA6*, *DNAJB1* and *CRYAB* genes were measured by quantitative RT-PCR analysis and normalized relative to β-actin mRNA. Protein expression levels were monitored by immunoblotting with the indicated antibodies in these and other figures. The levels of transcription in lane 1 were arbitrarily set at 1 in these and other figures. Error bars denote the standard deviations from three independent experiments in these and other figures.

chain reaction (RT-qPCR) (Figure 3B). Coexpression of eEF1BδL and RNF20/40 resulted in large increases in the expression of mRNA for all tested genes compared with that induced by eEF1BδL expression alone (Figure 3B, lane 3 versus lane 2). In contrast, coexpression of the eEF1BδL K381R mutant resulted in a much smaller induction of mRNA for heat shock-responsive genes (Figure 3B, lane 5 versus lane 3), suggesting an eEF1BδL monoubiquitylation-dependent coactivator function of RNF20/40. Furthermore, we found that heat-induced heat shock-responsive gene expression (Figure 3B, lane 6 versus lane 1) was increased by eEF1BδL expression (Figure 3B, lane 7) and was further enhanced by simultaneous expression of eEF1BδL and RNF20/40 (Figure 3B, lane 8). Increases in heat shock-dependent transcription are likely attributable to induction of heat shock-responsive transcription factors (36–38), which include eEF1BδL (Supplementary Figure S3A). Interestingly, we further found that RNF20/40-dependent eEF1BδL monoubiquitylation was also increased by heat shock treatment (Supplementary Figure S3B and C), suggesting that heat-induced eEF1BδL monoubiquitylation may also contribute somewhat to the observed increase in gene expression under thermal stress.

Next, we examined the role of endogenous RNF20 in the expression of heat shock-responsive genes in cells. RNF20 siRNA, which effectively decreased both RNF20 and RNF40, but not eEF1BδL, protein levels (Supplementary Figure S2I), significantly reduced the degree of eEF1BδL-dependent transcriptional activation of *DNAJB1*

and *CRYAB* genes, while causing little change in expression of the *HSPA6* gene (Figure 3C, lane 4 versus lane 2); it also markedly decreased heat shock-induced expression of all tested genes (Figure 3C, lane 7 versus lane 5 and lane 8 versus lane 6). As expected from concomitant decreases in RNF20 and RNF40 by RNF20 or RNF40 siRNA treatments (Supplementary Figure S2I), we obtained almost same results in a similar approach with RNF40 siRNA (Supplementary Figure S3D). Taken together, these results indicate that RNF20/40 acts through monoubiquitylation of eEF1BδL to function as a coactivator in the transcription of heat shock-responsive genes.

Notably, coexpression of RNF20/40 and eEF1BδL K381R consistently caused moderately higher transcription compared with expression of eEF1BδL K381R alone (Figure 3A, lane 8 versus lane 4, Figure 3B, lane 5 versus lane 4 and lane 10 versus lane 9). Similarly, RNF20ΔR/40ΔR expression also moderately enhanced eEF1BδL-dependent transcription (Figure 3A, lane 10 versus lane 2). These suggest the possibility that RNF20/40 may also influence eEF1BδL-mediated transcription in an eEF1BδL ubiquitylation-independent manner (see below).

RNF20/40 enhances recruitment of eEF1BδL to the promoter regions of heat shock-responsive genes

To elucidate the underlying mechanism by which RNF20/40 regulates eEF1BδL-mediated transcription of heat shock-responsive genes, we first examined whether RNF20/40 affects recruitment of eEF1BδL to its target genes. To this end, we transiently co-transfected 293T cells with RNF20 and RNF40 expression plasmids, with or without heat shock treatment, and performed chromatin immunoprecipitation (ChIP) assays to measure accumulation of eEF1BδL around the promoter regions of *HSPA6*, *DNAJB1* and *CRYAB* genes, which contain several HSEs proximal to their transcription start sites (Figure 4A). This analysis showed that RNF20/40 overexpression substantially increased eEF1BδL recruitment to the *CRYAB* gene, while having little effect on recruitment to *HSPA6* and *DNAJB1* genes (Figure 4B, lane 2 versus lane 1). Thermal stress resulted in a significant increase in eEF1BδL recruitment to the *HSPA6* gene, consistent with a previous report (17), as well as *DNAJB1* and *CRYAB* genes (Figure 4B, lane 3 versus lane 1). RNF20/40 overexpression combined with heat shock treatment resulted in a further enhancement in eEF1BδL accumulation (Figure 4B, lane 4 versus lane 3). To test whether the enhanced recruitment of eEF1BδL is caused by monoubiquitylation, we transiently transfected 293T cells with an expression plasmid for HA-tagged eEF1BδL wild-type or K381R mutant and performed a ChIP analysis using an anti-HA antibody. The eEF1BδL K381R mutant showed much less accumulation relative to wild-type eEF1BδL, both without heat shock treatment (Figure 4C, lane 2 versus lane 1 and lane 4 versus lane 3) and with heat shock treatment (Figure 4C, lane 6 versus lane 5 and lane 8 and lane 7). ChIP analyses further showed that siRNA-mediated RNF20 (Figure 4D, lane 2 versus lane 1 and lane 4 versus lane 3) and RNF40 (Figure S4) knockdown significantly reduced eEF1BδL accumulation at all tested promoter regions. Collectively, these results demonstrate that RNF20/40-dependent ubiquitylation of eEF1BδL potentiates eEF1BδL accumulation at the promoter regions of heat shock-responsive genes.

Monoubiquitylated eEF1BδL acts through direct interaction to recruit p-TEFb to the promoter regions of heat shock-responsive genes

Having established that RNF20/40-dependent ubiquitylation increases recruitment of eEF1BδL to target gene promoters, we sought to elucidate the specific mechanism by which eEF1BδL stimulates heat shock-responsive transcription. It has been reported that the release of promoter-proximal–paused RNA polymerase II to continue its elongation functions is a major limiting step in the transcription of heat shock-responsive genes (35,39–41). Notably, it has also been reported that p-TEFb, a transcription elongation factor composed of CDK9 and Cyclin T1 subunits, is rapidly recruited to heat shock loci and that recruitment of p-TEFb is sufficient to activate transcription, even in the absence of thermal stress (42–44). Accordingly, we examined whether eEF1BδL affects the recruitments of p-TEFb to the promoter regions of heat shock-responsive genes. ChIP analyses using an anti-CDK9 antibody showed that eEF1BδL depletion (Supplementary Figure S5A) decreased enrichment of CDK9 in the presence and absence of heat shock treatment (Figure 5A, lane 4 versus lane 3 and lane 2 versus lane 1). GST pull-down assays using purified p-TEFb (Supplementary Figure S5B) and eEF1BδL revealed that these proteins directly interact (Figure 5B) and further verified that amino acid residues 181–367 of eEF1BδL are responsible for the interaction with p-TEFb (Supplementary Figure S5C). These results indicate that eEF1BδL contributes to the efficient recruitment of p-TEFb to target gene promoters through direct protein interaction.

It has been reported that monoubiquitylation of the acidic region of transcription factors provides a preferential binding platform for p-TEFb, thereby enhancing transcription elongation rates (45,46). Notably, we found that the isoelectric value (pI) of the 12 amino acid residues around the K381 eEF1BδL ubiquitylation site (Supplementary Figure S5D) is about 4.2; thus, this region has the potential to create an acidic environment. Accordingly, we examined whether RNF20/40-mediated eEF1BδL monoubiquitylation affects p-TEFb recruitment to target gene promoters. Our ChIP analysis showed that RNF20/40 expression increased recruitment of CDK9 under thermal stress condition (Figure 5C, lane 4 versus lane 3), although this effect of RNF20/40 was relatively modest at *HSPA6* and *DNAJB1* gene promoters in the absence of heat shock (Figure 5C, lane 2 versus lane 1). In addition, in a test for CDK9 recruitment to the promoter region of *PMS2* gene that was previously reported as a CDK9 target gene (47) but almost irresponsive to eEF1BδL, HSF1 and RNF20/40 expressions or heat shock (Supplementary Figure S5E), we found that thermal stress and RNF20/40 expression did not much affect recruitment of CDK9 at the *PMS2* gene promoter (Supplementary Figure S5F). We further found that coexpression of RNF20/40 and eEF1BδL markedly increased CDK9 recruitment relative to that induced by eEF1BδL expression alone (Figure 5D, lane 3 versus lane 1 and lane 7

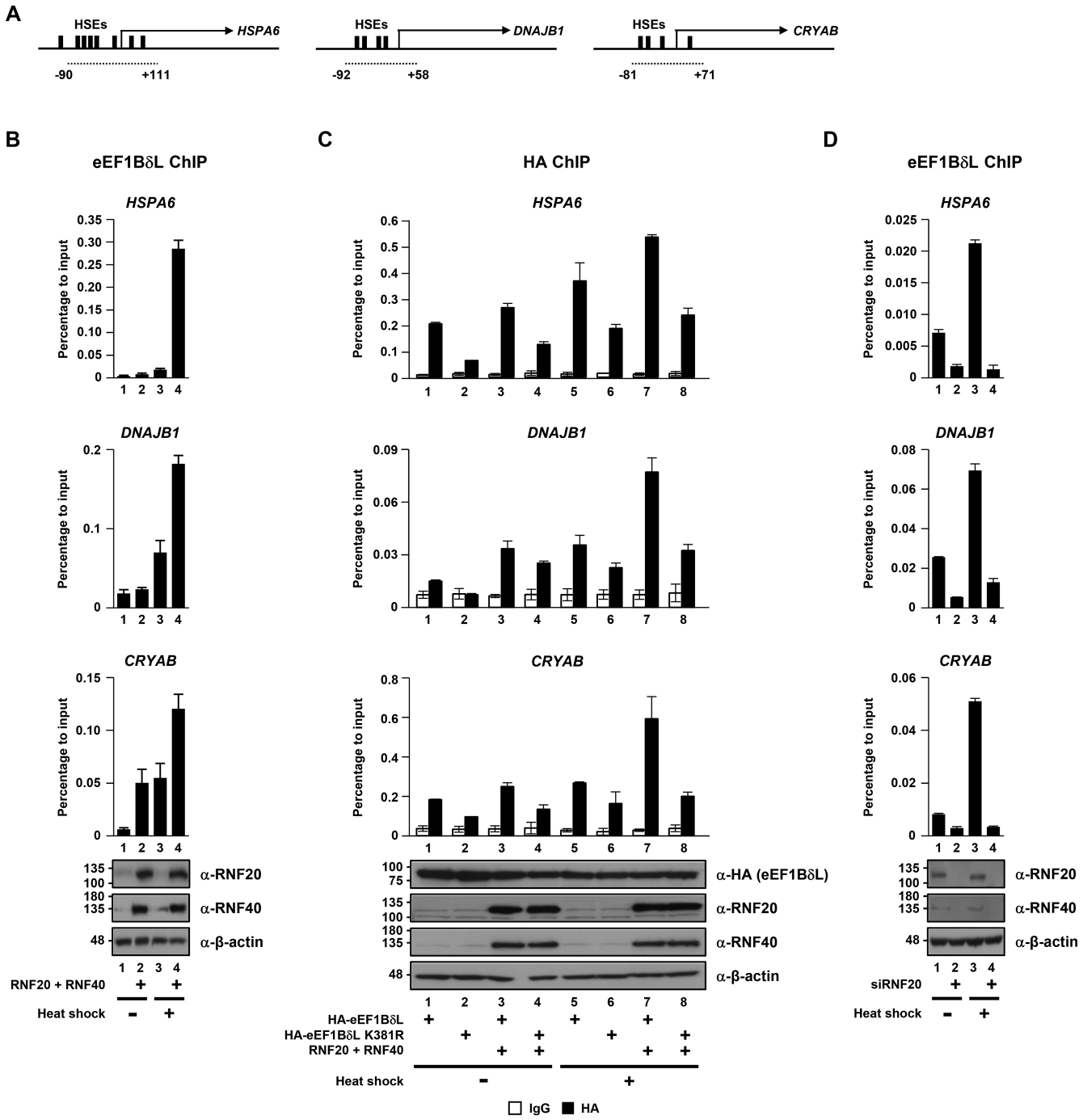

Figure 4. RNF20/40 enhances recruitment of eEF1BδL to the promoter regions of heat shock-responsive genes. (**A**) Schematic representation of the *HSPA6*, *DNAJB1* and *CRYAB* loci and amplicons (dotted lines) used for quantitative PCR. Black bars indicate HSEs. Numbers below the amplicons indicate base pairs from the transcription start site of the gene. (**B**–**D**) Accumulation of eEF1BδL around the promoter regions of heat shock-responsive genes. 293T cells were co-transfected with indicated protein expression plasmids (B and C) or treated with RNF20-targeted siRNA (D). After heat shock treatment where indicated, chromatin immunoprecipitation (ChIP) analyses were performed with anti-eEF1BδL (B and D) or anti-HA (C) antibodies. Anti-rabbit IgG was used as a control in (C). Error bars denote the standard deviations from two independent experiments in these and other figures.

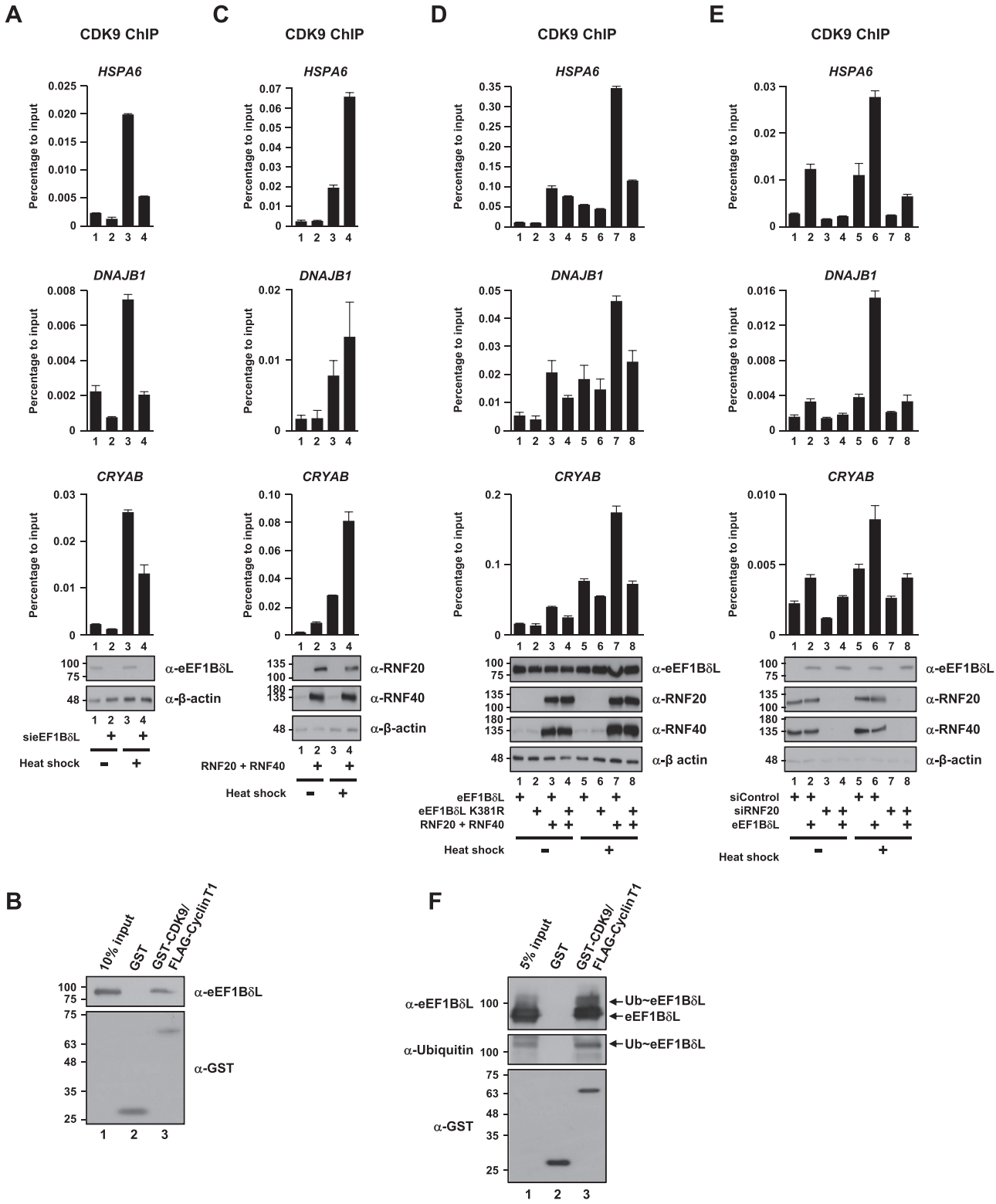

Figure 5. Monoubiquitylated eEF1BδL acts through direct interaction to recruit p-TEFb to the promoter regions of heat shock-responsive genes. (**A**, **C**, **D** and **E**) Accumulation of CDK9 around the promoter regions of heat shock-responsive genes. 293T cells were treated with either control or eEF1BδL-targeted (sieEF1BδL) siRNAs (A), either control or RNF20-targeted siRNAs (E), and transfected with eEF1BδL expression plasmid (E) as indicated. 293T cells were co-transfected with indicated protein expression plasmids (C and D). After heat shock treatment where indicated, ChIP analyses were performed with anti-CDK9 antibody. (**B**) Direct binding of eEF1BδL to p-TEFb. GST pull-down assays employed purified p-TEFb (GST-CDK9/FLAG-Cyclin T1) (Supplementary Figure S5B) and FLAG-eEF1BδL. (**F**) Enhanced binding of monoubiquitylated eEF1BδL to p-TEFb. FLAG-eEF1BδL was ubiquitylated *in vitro* using purified factors as in Figure 2 and then tested for binding to purified p-TEFb.

versus lane 5); however, this RNF20/40-dependent increase in recruitment was diminished upon coexpression with the eEF1BδL K381R mutant (Figure 5D, lane 4 versus lane 3 and lane 8 versus lane 7). We also found that eEF1BδL-induced CDK9 recruitment was attenuated by depletions of RNF20 (Figure 5E, lane 4 versus lane 2 and lane 8 versus lane 6) and RNF40 (Supplementary Figure S5G).

To more directly assess the effect of eEF1BδL monoubiquitylation on eEF1BδL–p-TEFb interactions, we first ubiquitylated purified eEF1BδL using purified factors *in vitro*, as shown in Figure 2, and then performed protein-interaction assays using purified p-TEFb. This analysis showed that p-TEFb interacts more efficiently with ubiquitylated eEF1BδL than with the non-ubiquitylated species (Figure 5F). Taken together, these results suggest that RNF20/40-mediated monoubiquitylation of eEF1BδL potentiates recruitment of the transcription elongation factor p-TEFb to the promoter regions of heat shock-responsive genes and thereby stimulates the release of promoter-proximal–paused RNA polymerase II, allowing it to perform its elongation functions.

Cooperative binding of eEF1BδL, RNF20/40 and HSF1 synergistically enhances the expression of heat shock-responsive genes

The eEF1BδL K381R mutant consistently promoted enhanced heat shock-responsive gene expression when co-expressed with RNF20/40, albeit to a lesser extent than wild-type eEF1BδL (Figure 3). This suggests that eEF1BδL and RNF20/40, possibly in conjunction with other heat shock transcription factor(s), affects transcription in an ubiquitylation-independent manner. Therefore, given that eEF1BδL directly interacts with RNF20/40 and eEF1BδL co-immunoprecipitates with HSF1 (heat shock factor 1) (17), a master heat shock regulator (36,38,48), we postulated that eEF1BδL, RNF20/40, and HSF1 act coordinately in regulating heat shock-responsive gene expression. In support of this, we found that endogenous eEF1BδL, RNF20, and HSF1 proteins co-immunoprecipitated with each other (Supplementary Figure S6A). Furthermore, protein-interaction studies using purified HSF1 (Supplementary Figure S6B) revealed that HSF1 directly interacts with RNF20/40 as well as eEF1BδL (Figure 6A) through amino acid residues 181–367 of eEF1BδL (Supplementary Figure S6C). Importantly, we also found that the direct interaction between eEF1BδL and HSF1 was markedly enhanced by addition of purified RNF20/40 (Figure 6B, top, lane 5 versus lane 3). In a test of intracellular binding, the interaction between eEF1BδL and HSF1 was also strengthened by overexpression of RNF20/40 in the presence of thermal stress (Figure 6C, top, lane 12 versus lane 9) and in its absence (Figure 6C, top, lane 6 versus lane 3). In addition, this cooperative binding was independent of RNF20/40-mediated eEF1BδL ubiquitylation (Figure 6D, top, lane 6 versus lane 8). Collectively, these results indicate direct and cooperative interactions among eEF1BδL, RNF20/40, and HSF1. Notably, the ubiquitylation-independent cooperative binding explains, at least in part, why the eEF1BδL K381R mutant moderately enhanced heat shock-responsive gene expression in the presence of RNF20/40 (Figure 3).

Consistent with the protein-interaction studies described above, we found that eEF1BδL, HSF1, RNF20 and CDK9 were all localized to the promoter regions of heat shock-responsive genes, but not to the intergenic region downstream of the *HSPA6* gene, and that their enrichment was markedly enhanced by heat shock treatment (Supplementary Figure S6D). As was the case for eEF1BδL (Figure 4D, Supplementary Figure S4), RNF20 (Figure 6E) and RNF40 (Supplementary Figure S6E) depletions resulted in decreased HSF1 occupancy on the promoter regions of these genes. Thus, these results indicate that RNF20/40 enhances the targeting of both eEF1BδL and HSF1 to target gene promoter regions. Finally, given the cooperative physical interaction and colocalization of eEF1BδL, RNF20/40 and HSF1 on chromatin, we tested the synergistic effect of these proteins on heat shock-responsive gene expression. This analysis showed that coexpression of eEF1BδL, RNF20/40, and HSF1 resulted in higher expression of the *HSPA6* gene compared with that produced by individual or paired expression of these proteins in the presence (Figure 6F, lane 16) or absence (Figure 6F, lane 8) of thermal stress. Similar results were observed for *DNAJB1* and *CRYAB* genes (Supplementary Figure S6F). Collectively, these results suggest that eEF1BδL, RNF20/40, and HSF1 act synergistically through their cooperative interactions to enhance the expression of heat shock-responsive genes.

DISCUSSION

Defects in RNF20 cause cell-cycle arrest, genomic instability and apoptosis (10,16), emphasizing the importance of this E3 ubiquitin ligase in cell survival. On a related note, accumulating evidence has implicated RNF20 in tumorigenesis (49–51). Based on recent reports that many histone-modifying enzymes target non-histone proteins that play important roles in various cellular events (52), it is reasonable that RNF20/40 might also have additional ubiquitylation target protein(s) other than histone H2B that are important for cell viability. This supposition is supported by recent studies that have reported several non-histone ubiquitylation target proteins of RNF20/40 (13–16).

Starting with forward screening of RNF20/40-interacting proteins, we used *in vitro* ubiquitylation assays employing defined purified factors in conjunction with confirming cellular analyses to unequivocally demonstrate that RNF20/40 monoubiquitylates eEF1BδL together with its cognate E2 ubiquitin-conjugating enzyme, RAD6A. RAD6 also serves as an E2 enzyme for RAD18. From a mechanistic standpoint, RAD6 promotes polyubiquitylation by binding free ubiquitin non-covalently through its backside surface (53). However, it has been reported that RAD18 directs RAD6-mediated monoubiquitylation of a specific site in PCNA by blocking the backside of RAD6 (29). Interestingly, our structural analysis of the complexed form of Bre1 and Rad6 (yeast homologs of RNF20/40 and RAD6, respectively) also revealed that the N-terminal region of Bre1 is anchored to the backside of Rad6 and mediates E2 recognition (unpublished data). Assuming that this structural feature also applies to the human homologs,

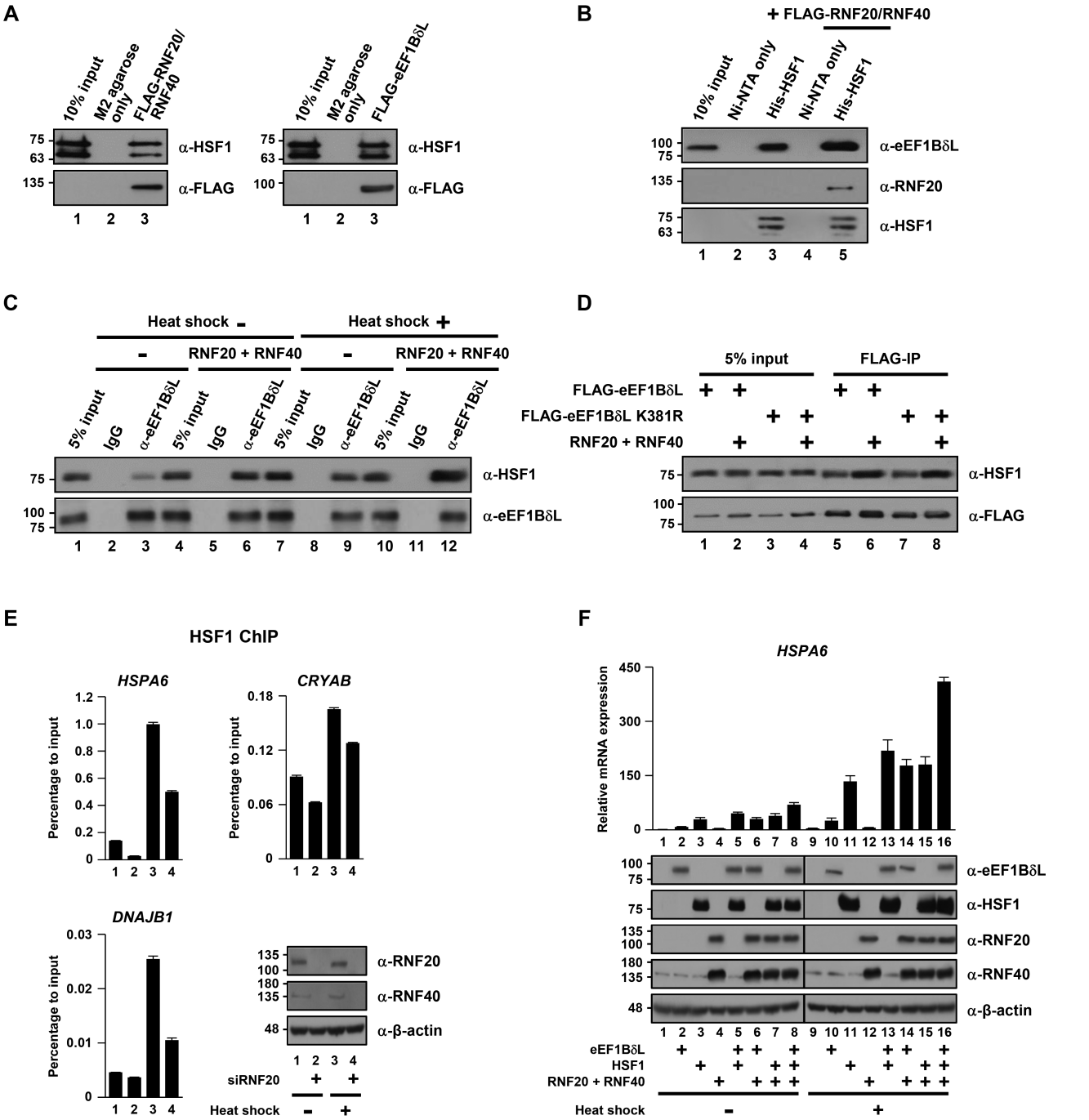

Figure 6. Cooperative binding of eEF1BδL, RNF20/40 and HSF1 synergistically enhances the expression of heat shock-responsive genes. (**A**) Direct bindings of HSF1 to RNF20/40 and eEF1BδL. Purified His-HSF1 (Supplementary Figure S6B) was tested for binding to M2 agarose-coupled FLAG-RNF20/RNF40 (left) and FLAG-eEF1BδL (right). (**B**) Cooperative interactions among eEF1BδL, RNF20/40 and HSF1 *in vitro*. Purified FLAG-eEF1BδL was tested for binding to Ni-NTA agarose-coupled His-HSF1 in the presence (lanes 4 and 5) and in the absence (lanes 2 and 3) of FLAG-RNF20/RNF40. (**C** and **D**) Cooperative interactions among eEF1BδL, RNF20/40 and HSF1 in cells. 293T cells were co-transfected with RNF20 and RNF40 expression plasmids, followed with heat shock treatment where indicated, and cell extracts were co-immunoprecipitated with anti-eEF1BδL antibody (C). 293T cells were co-transfected with indicated protein expression plasmids. Cell extracts were immunoprecipitated with anti-FLAG antibody (D). The bound proteins were scored by immunoblotting with the indicated antibodies. (**E**) Effect of endogenous RNF20 on recruitment of HSF1 to the promoter regions of heat shock-responsive genes. 293T cells were treated with RNF20-targeted siRNA, followed with heat shock treatment where indicated, and ChIP analyses were performed using anti-HSF1 antibody. Note that same cell lysates were used in the experiments for this figure and Figure 4D. (**F**) Synergistic effect of eEF1BδL, RNF20/40 and HSF1 on transcription of the *HSPA6* gene. 293T cells were co-transfected with indicated combinations of protein expression plasmids, followed with heat shock treatment where indicated, and mRNA levels of the *HSPA6* gene were analyzed.

RNF20/40–RAD6 would mediate ubiquitylation of target proteins in a monoubiquitylation manner. This would explain why RNF20/40–RAD6 mediates monoubiquitylation, rather than polyubiquitylation, of histone H2B (8), Eg5 (16) and eEF1BδL, a modification that exerts non-proteolytic functions (2,3) instead of directing the proteins for proteasome-mediated degradation.

Hyperthermia immediately induces the expression of heat shock proteins (35,54), many of which are molecular chaperones that serve to maintain protein quality (55). Prior to induction by heat, a significant fraction of RNA polymerase II is already engaged at promoter-proximal regions of target genes, allowing for a rapid response to stimulation (56). Early studies in *Drosophila* found that the rapid induction of heat shock-responsive genes is largely dependent on HSF1 (57). Upon an elevation in temperature, HSF1 translocates into the nucleus, binds to HSEs, and recruits p-TEFb to facilitate the release of RNA polymerase II from its paused state and convert it to an elongating state. A subsequent study showed that HSF1 alone is not sufficient to provoke p-TEFb–mediated transcriptional activation (42), suggesting the presence of additional factors that can compensate for and/or synergize with HSF1 to fully support the recruitment and action of p-TEFb. One such additional heat shock transcription factor candidate is eEF1BδL. It was first reported that eEF1BδL protein level is substantially increased in response to thermal stress and translocates into the nucleus, where it upregulates heat shock-responsive genes in cooperation with HSF1 (17). But how eEF1BδL exerts its role in regulating heat shock-responsive gene expression has not been established.

Our biochemical and cellular analyses provide valuable insight into the molecular mechanism underlying eEF1BδL regulation of heat shock-responsive gene expression, showing that eEF1BδL functions are modulated by RNF20/40 (Figure 7). We propose that RNF20/40-mediated monoubiquitylation of eEF1BδL increases eEF1BδL accumulation at HSE-containing promoter regions, and thus enhances transcription of heat shock-responsive genes. Although it is not clear whether monoubiquitylation directly increases the affinity of eEF1BδL for HSE, our studies provide direct evidence that eEF1BδL monoubiquitylation contributes to heat shock-responsive gene expression by enhancing the recruitment of p-TEFb through physical interaction of monoubiquitylated eEF1BδL with p-TEFb. Importantly, in addition to monoubiquitylation of transcription factors (45), RNF20/40- (58) and MLS-mediated (59) histone H2B monoubiquitylation have also been implicated in the recruitment and stabilization of p-TEFb at active gene promoters, supporting pivotal roles of monoubiquitylation of transcription factors and nucleosome components in early transcription-elongation events. Apart from the ubiquitylation-dependent functions of eEF1BδL, we also envision that RNF20/40 and eEF1BδL contribute to heat shock-responsive transcription via an ubiquitylation-independent pathway. Our demonstration that eEF1BδL, RNF20/40 and HSF1 interact, and that RNF20/40 strengthens the physical interaction between eEF1BδL and HSF1, collectively suggest that these players are cooperatively stabilized and accumulate on promoter regions of heat shock-responsive genes, leading to increased p-TEFb recruitment and transcriptional activation. In addition, we found that the physical interaction between HSF1 and p-TEFb is strengthened by eEF1BδL (Supplementary Figure S7A), highlighting the role of eEF1BδL, in cooperation with HSF1, in the transcription of heat shock-responsive genes. We further found that neither HSF1 nor eEF1BδL can rescue transcriptional activation in the absence of the other (Supplementary Figure S7B–D), suggesting that eEF1BδL and HSF1 synergize to serve non-redundant functions in promoting target gene expression. The N-terminal part of eEF1BδL (amino acid residues 1–367) is unique to eEF1BδL and is not present in the cytoplasmic eEF1Bδ1 isoform. Interestingly, we found that RNF20/40, p-TEFb, and HSF1 all bind to the N-terminal region of eEF1BδL. A previous report showed that the N-terminal region of eEF1BδL alone is unable to support transcriptional activity (17). These results help define the molecular architecture of eEF1BδL as a transcription activator: the N-terminal region is responsible for binding to the HSE (17) and also provides a binding platform for cooperative interactions with transcription factors, whereas the C-terminal region plays a role in the transactivation activity of eEF1BδL.

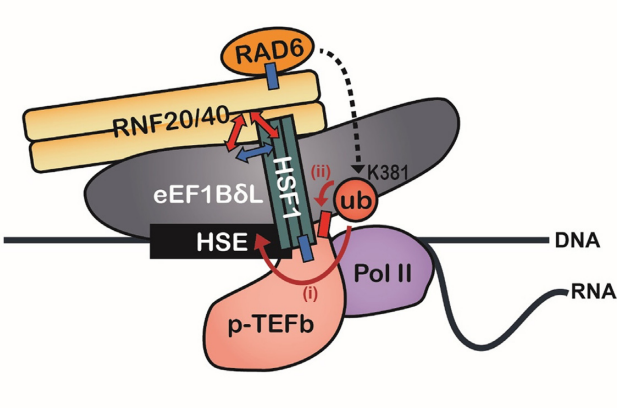

Figure 7. Mechanistic model of RNF20/40-mediated expression of heat shock genes through eEF1BδL monoubiquitylation and cooperative protein interactions. Ubiquitylation-dependent mechanism: We propose that RNF20/40–RAD6 monoubiquitylates eEF1BδL at lysine 381, which in turn potentiates recruitment of (i) eEF1BδL itself and (ii) p-TEFb through direct interactions of monoubiquitylated eEF1BδL to HSE-containing promoter regions of heat shock-responsive genes. Ubiquitylation-independent mechanism: A direct interaction of eEF1BδL with RNF20/40 results in cooperative binding to HSF1 (depicted by thick arrows) and a synergistic effect on transcription. Protein interactions verified in this and previous studies are depicted by red and blue color, respectively.

Although heat shock-responsive transcriptional regulation has been extensively studied in *Drosophila*, eEF1BδL has not been recognized as an important heat shock-responsive transcription factor in *Drosophila*. Notable in this context, the eEF1BδL isoform is unique to mammalian cells, and is not expressed in *Drosophila* (60). Our study thus provides a novel molecular mechanism to explain how mammalian-specific eEF1BδL functions in heat shock-responsive transcription in collaboration with HSF1, and add important additional information to account for pre-

vious observations that HSF1 alone is not sufficient for recruitment of p-TEFb to the promoters of target genes.

These mechanistic insights into eEF1BδL monoubiquitylation provide another example of the non-proteolytic function of RNF20/40-mediated protein ubiquitylation in addition to its established function in ubiquitylating histone H2B (61,62) and shed light on the role of multiple players in orchestrating stress-responsive gene expression (63).

SUPPLEMENTARY DATA

Supplementary Data are available at NAR Online.

ACKNOWLEDGEMENTS

We thank Dr. Masayuki Matsushita for eEF1BδL, HSF1 and luciferase reporter plasmids.

FUNDING

National Research Foundation of Korea [NRF-2015R1A1A1A05001593 and NRF-2018R1A5A1024261 to J.K.]; National Research Council of Science and Technology [DRC-14-2-KRISS to J.E.L.]. Funding for open access charge: National Research Foundation of Korea [NRF-2018R1A5A1024261].
Conflict of interest statement. None declared.

REFERENCES

1. Pickart,C.M. (2001) Mechanisms underlying ubiquitination. *Annu. Rev. Biochem.*, **70**, 503–533.
2. Geng,F., Wenzel,S. and Tansey,W.P. (2012) Ubiquitin and proteasomes in transcription. *Annu. Rev. Biochem.*, **81**, 177–201.
3. Nakagawa,T. and Nakayama,K. (2015) Protein monoubiquitylation: targets and diverse functions. *Genes Cells*, **20**, 543–562.
4. Kaiser,S.E., Riley,B.E., Shaler,T.A., Trevino,R.S., Becker,C.H., Schulman,H. and Kopito,R.R. (2011) Protein standard absolute quantification (PSAQ) method for the measurement of cellular ubiquitin pools. *Nat. Methods*, **8**, 691–696.
5. Sigismund,S., Polo,S. and Di Fiore,P.P. (2004) Signaling through monoubiquitination. *Curr. Top. Microbiol. Immunol.*, **286**, 149–185.
6. Kim,W., Bennett,E.J., Huttlin,E.L., Guo,A., Li,J., Possemato,A., Sowa,M.E., Rad,R., Rush,J., Comb,M.J. *et al.* (2011) Systematic and quantitative assessment of the ubiquitin-modified proteome. *Mol. Cell*, **44**, 325–340.
7. Zhu,B., Zheng,Y., Pham,A.D., Mandal,S.S., Erdjument-Bromage,H., Tempst,P. and Reinberg,D. (2005) Monoubiquitination of human histone H2B: the factors involved and their roles in *HOX* gene regulation. *Mol. Cell*, **20**, 601–611.
8. Kim,J., Guermah,M., McGinty,R.K., Lee,J.S., Tang,Z., Milne,T.A., Shilatifard,A., Muir,T.W. and Roeder,R.G. (2009) RAD6-mediated transcription-coupled H2B ubiquitylation directly stimulates H3K4 methylation in human cells. *Cell*, **137**, 459–471.
9. Shema,E., Tirosh,I., Aylon,Y., Huang,J., Ye,C., Moskovits,N., Raver-Shapira,N., Minsky,N., Pirngruber,J., Tarcic,G. *et al.* (2008) The histone H2B-specific ubiquitin ligase RNF20/hBRE1 acts as a putative tumor suppressor through selective regulation of gene expression. *Genes Dev.*, **22**, 2664–2676.
10. Chernikova,S.B., Razorenova,O.V., Higgins,J.P., Sishc,B.J., Nicolau,M., Dorth,J.A., Chernikova,D.A., Kwok,S., Brooks,J.D., Bailey,S.M. *et al.* (2012) Deficiency in mammalian histone H2B ubiquitin ligase Bre1 (Rnf20/Rnf40) leads to replication stress and chromosomal instability. *Cancer Res.*, **72**, 2111–2119.
11. Tarcic,O., Pateras,I.S., Cooks,T., Shema,E., Kanterman,J., Ashkenazi,H., Boocholez,H., Hubert,A., Rotkopf,R., Baniyash,M. *et al.* (2016) RNF20 links histone H2B ubiquitylation with inflammation and inflammation-associated cancer. *Cell Rep.*, **14**, 1462–1476.
12. Foster,E.R. and Downs,J.A. (2009) Methylation of H3 K4 and K79 is not strictly dependent on H2B K123 ubiquitylation. *J. Cell Biol.*, **184**, 631–638.
13. Liu,Z., Oh,S.M., Okada,M., Liu,X., Cheng,D., Peng,J., Brat,D.J., Sun,S.Y., Zhou,W., Gu,W. *et al.* (2009) Human BRE1 is an E3 ubiquitin ligase for Ebp1 tumor suppressor. *Mol. Biol. Cell*, **20**, 757–768.
14. Lee,J.H., Lee,G.Y., Jang,H., Choe,S.S., Koo,S.H. and Kim,J.B. (2014) Ring finger protein20 regulates hepatic lipid metabolism through protein kinase A-dependent sterol regulatory element binding protein1c degradation. *Hepatology*, **60**, 844–857.
15. Ren,P., Sheng,Z., Wang,Y., Yi,X., Zhou,Q., Zhou,J., Xiang,S., Hu,X. and Zhang,J. (2014) RNF20 promotes the polyubiquitination and proteasome-dependent degradation of AP-2α protein. *Acta Biochim. Biophys. Sin. (Shanghai)*, **46**, 136–140.
16. Duan,Y., Huo,D., Gao,J., Wu,H., Ye,Z., Liu,Z., Zhang,K., Shan,L., Zhou,X., Wang,Y. *et al.* (2016) Ubiquitin ligase RNF20/40 facilitates spindle assembly and promotes breast carcinogenesis through stabilizing motor protein Eg5. *Nat. Commun.*, **7**, 12648.
17. Kaitsuka,T., Tomizawa,K. and Matsushita,M. (2011) Transformation of eEF1Bδ into heat-shock response transcription factor by alternative splicing. *EMBO Rep.*, **12**, 673–681.
18. Kim,J. and Roeder,R.G. (2011) Nucleosomal H2B ubiquitylation with purified factors. *Methods*, **54**, 331–338.
19. Rappsilber,J., Mann,M. and Ishihama,Y. (2007) Protocol for micro-purification, enrichment, pre-fractionation and storage of peptides for proteomics using StageTips. *Nat. Protoc.*, **2**, 1896–1906.
20. Cox,J. and Mann,M. (2008) MaxQuant enables high peptide identification rates, individualized p.p.b.-range mass accuracies and proteome-wide protein quantification. *Nat. Biotechnol.*, **26**, 1367–1372.
21. Schwanhausser,B., Busse,D., Li,N., Dittmar,G., Schuchhardt,J., Wolf,J., Chen,W. and Selbach,M. (2011) Global quantification of mammalian gene expression control. *Nature*, **473**, 337–342.
22. Bustin,S.A., Benes,V., Garson,J.A., Hellemans,J., Huggett,J., Kubista,M., Mueller,R., Nolan,T., Pfaffl,M.W., Shipley,G.L. *et al.* (2009) The MIQE guidelines: minimum information for publication of quantitative real-time PCR experiments. *Clin. Chem.*, **55**, 611–622.
23. Kim,J., Hake,S.B. and Roeder,R.G. (2005) The human homolog of yeast BRE1 functions as a transcriptional coactivator through direct activator interactions. *Mol. Cell*, **20**, 759–770.
24. Zhang,F. and Yu,X. (2011) WAC, a functional partner of RNF20/40, regulates histone H2B ubiquitination and gene transcription. *Mol. Cell*, **41**, 384–397.
25. Le Sourd,F., Boulben,S., Le Bouffant,R., Cormier,P., Morales,J., Belle,R. and Mulner-Lorillon,O. (2006) eEF1B: At the dawn of the 21st century. *Biochim. Biophys. Acta*, **1759**, 13–31.
26. Andersen,G.R., Nissen,P. and Nyborg,J. (2003) Elongation factors in protein biosynthesis. *Trends Biochem. Sci.*, **28**, 434–441.
27. Jentsch,S., McGrath,J.P. and Varshavsky,A. (1987) The yeast DNA repair gene *RAD6* encodes a ubiquitin-conjugating enzyme. *Nature*, **329**, 131–134.
28. Kim,J. and Roeder,R.G. (2009) Direct Bre1-Paf1 complex interactions and RING finger-independent Bre1-Rad6 interactions mediate histone H2B ubiquitylation in yeast. *J. Biol. Chem.*, **284**, 20582–20592.
29. Hibbert,R.G., Huang,A., Boelens,R. and Sixma,T.K. (2011) E3 ligase Rad18 promotes monoubiquitination rather than ubiquitin chain formation by E2 enzyme Rad6. *Proc. Natl. Acad. Sci. U.S.A.*, **108**, 5590–5595.
30. Wagner,S.A., Beli,P., Weinert,B.T., Nielsen,M.L., Cox,J., Mann,M. and Choudhary,C. (2011) A proteome-wide, quantitative survey of in vivo ubiquitylation sites reveals widespread regulatory roles. *Mol. Cell. Proteomics*, **10**, M111.013284.
31. Povlsen,L.K., Beli,P., Wagner,S.A., Poulsen,S.L., Sylvestersen,K.B., Poulsen,J.W., Nielsen,M.L., Bekker-Jensen,S., Mailand,N. and Choudhary,C. (2012) Systems-wide analysis of ubiquitylation dynamics reveals a key role for PAF15 ubiquitylation in DNA-damage bypass. *Nat. Cell Biol.*, **14**, 1089–1098.
32. Greer,S.F., Zika,E., Conti,B., Zhu,X.S. and Ting,J.P. (2003) Enhancement of CIITA transcriptional function by ubiquitin. *Nat. Immunol.*, **4**, 1074–1082.
33. Head,M.W., Hurwitz,L. and Goldman,J.E. (1996) Transcription regulation of alpha B-crystallin in astrocytes: analysis of HSF and

AP1 activation by different types of physiological stress. *J. Cell Sci.*, **109**, 1029–1039.
34. Trinklein,N.D., Murray,J.I., Hartman,S.J., Botstein,D. and Myers,R.M. (2004) The role of heat shock transcription factor 1 in the genome-wide regulation of the mammalian heat shock response. *Mol. Biol. Cell*, **15**, 1254–1261.
35. Mahat,D.B., Salamanca,H.H., Duarte,F.M., Danko,C.G. and Lis,J.T. (2016) Mammalian heat shock response and mechanisms underlying its genome-wide transcriptional regulation. *Mol. Cell*, **62**, 63–78.
36. Akerfelt,M., Morimoto,R.I. and Sistonen,L. (2010) Heat shock factors: integrators of cell stress, development and lifespan. *Nat. Rev. Mol. Cell Biol.*, **11**, 545–555.
37. Anckar,J. and Sistonen,L. (2011) Regulation of HSF1 function in the heat stress response: implications in aging and disease. *Annu. Rev. Biochem.*, **80**, 1089–1115.
38. Gomez-Pastor,R., Burchfiel,E.T. and Thiele,D.J. (2018) Regulation of heat shock transcription factors and their roles in physiology and disease. *Nat. Rev. Mol. Cell Biol.*, **19**, 4–19.
39. Teves,S.S. and Henikoff,S. (2013) The heat shock response: A case study of chromatin dynamics in gene regulation. *Biochem. Cell Biol.*, **91**, 42–48.
40. Bunch,H. (2017) RNA polymerase II pausing and transcriptional regulation of the *HSP70* expression. *Eur. J. Cell Biol.*, **96**, 739–745.
41. Vihervaara,A., Mahat,D.B., Guertin,M.J., Chu,T., Danko,C.G., Lis,J.T. and Sistonen,L. (2017) Transcriptional response to stress is pre-wired by promoter and enhancer architecture. *Nat. Commun.*, **8**, 255.
42. Lis,J.T., Mason,P., Peng,J., Price,D.H. and Werner,J. (2000) P-TEFb kinase recruitment and function at heat shock loci. *Genes Dev.*, **14**, 792–803.
43. Ni,Z., Saunders,A., Fuda,N.J., Yao,J., Suarez,J.R., Webb,W.W. and Lis,J.T. (2008) P-TEFb is critical for the maturation of RNA polymerase II into productive elongation in vivo. *Mol. Cell. Biol.*, **28**, 1161–1170.
44. Kwak,H. and Lis,J.T. (2013) Control of transcriptional elongation. *Annu. Rev. Genet.*, **47**, 483–508.
45. Muratani,M. and Tansey,W.P. (2003) How the ubiquitin-proteasome system controls transcription. *Nat. Rev. Mol. Cell Biol.*, **4**, 192–201.
46. Kurosu,T. and Peterlin,B.M. (2004) VP16 and ubiquitin; binding of P-TEFb via its activation domain and ubiquitin facilitates elongation of transcription of target genes. *Curr. Biol.*, **14**, 1112–1116.
47. Chen,L., Chen,J.Y., Huang,Y.J., Gu,Y., Qiu,J., Qian,H., Shao,C., Zhang,X., Hu,J., Li,H. *et al.* (2018) The augmented R-Loop is a unifying mechanism for myelodysplastic syndromes induced by high-risk splicing factor mutations. *Mol. Cell*, **69**, 412–425.
48. Zobeck,K.L., Buckley,M.S., Zipfel,W.R. and Lis,J.T. (2010) Recruitment timing and dynamics of transcription factors at the *Hsp70* loci in living cells. *Mol. Cell*, **40**, 965–975.
49. Shiloh,Y., Shema,E., Moyal,L. and Oren,M. (2011) RNF20-RNF40: A ubiquitin-driven link between gene expression and the DNA damage response. *FEBS Lett.*, **585**, 2795–2802.
50. Cole,A.J., Clifton-Bligh,R. and Marsh,D.J. (2015) Histone H2B monoubiquitination: roles to play in human malignancy. *Endocr. Relat. Cancer*, **22**, T19–T33.
51. Sethi,G., Shanmugam,M.K., Arfuso,F. and Kumar,A.P. (2018) Role of RNF20 in cancer development and progression - a comprehensive review. *Biosci. Rep.*, **38**, BSR20171287.
52. Buuh,Z.Y., Lyu,Z. and Wang,R.E. (2018) Interrogating the roles of post-translational modifications of non-histone proteins. *J. Med. Chem.*, **61**, 3239–3252.
53. Miura,T., Klaus,W., Gsell,B., Miyamoto,C. and Senn,H. (1999) Characterization of the binding interface between ubiquitin and class I human ubiquitin-conjugating enzyme 2b by multidimensional heteronuclear NMR spectroscopy in solution. *J. Mol. Biol.*, **290**, 213–228.
54. Richter,K., Haslbeck,M. and Buchner,J. (2010) The heat shock response: life on the verge of death. *Mol. Cell*, **40**, 253–266.
55. Chen,B., Retzlaff,M., Roos,T. and Frydman,J. (2011) Cellular strategies of protein quality control. *Cold Spring Harb. Perspect. Biol.*, **3**, a004374.
56. Adelman,K. and Lis,J.T. (2012) Promoter-proximal pausing of RNA polymerase II: emerging roles in metazoans. *Nat. Rev. Genet.*, **13**, 720–731.
57. Guertin,M.J., Petesch,S.J., Zobeck,K.L., Min,I.M. and Lis,J.T. (2010) Drosophila heat shock system as a general model to investigate transcriptional regulation. *Cold Spring Harb. Symp. Quant. Biol.*, **75**, 1–9.
58. Sanso,M., Lee,K.M., Viladevall,L., Jacques,P.E., Page,V., Nagy,S., Racine,A., St Amour,C.V., Zhang,C., Shokat,K.M. *et al.* (2012) A positive feedback loop links opposing functions of P-TEFb/Cdk9 and histone H2B ubiquitylation to regulate transcript elongation in fission yeast. *PLoS Genet.*, **8**, e1002822.
59. Wu,L., Li,L., Zhou,B., Qin,Z. and Dou,Y. (2014) H2B ubiquitylation promotes RNA Pol II processivity via PAF1 and pTEFb. *Mol. Cell*, **54**, 920–931.
60. Kaitsuka,T. and Matsushita,M. (2015) Regulation of translation factor EEF1D gene function by alternative splicing. *Int. J. Mol. Sci.*, **16**, 3970–3979.
61. Weake,V.M. and Workman,J.L. (2008) Histone ubiquitination: triggering gene activity. *Mol. Cell*, **29**, 653–663.
62. Fuchs,G. and Oren,M. (2014) Writing and reading H2B monoubiquitylation. *Biochim. Biophys. Acta*, **1839**, 694–701.
63. Xu,D., Zalmas,L.P. and La Thangue,N.B. (2008) A transcription cofactor required for the heat-shock response. *EMBO Rep.*, **9**, 662–669.